

1

1. Extended Data

Figure #	Figure title One sentence only	Filename This should be the name the file is saved as when it is uploaded to our system. Please include the file extension. i.e.: <i>Smith_ED</i> <i>Fig1.jpg</i>	Figure Legend If you are citing a reference for the first time in these legends, please include all new references in the Online Methods References section, and carry on the numbering from the main References section of the paper.
Extended Data Fig. 1	Study design	Extended Data Fig.1. Study design.tif	<p>We applied the multi-trait analysis of GWAS (MTAG) algorithm to datasets of European descent (unless otherwise specified). a, We applied MTAG to four datasets (glaucoma case-control GWAS from the UKBB; GWAS meta-analysis of intraocular pressure (IOP) from the International Glaucoma Genetics Consortium (IGGC) and the UKBB; Vertical cup-disc ratio (VCDR) GWAS data that was either adjusted for vertical disc diameter (VDD) in the UKBB dataset; or not adjusted for VDD in the IGGC). Novel variants identified through this analysis were then confirmed in two independent data sets: an Australasian cohort of advanced glaucoma (ANZRAG) and a consortium of cohorts from the United States (NEIGHBORHOOD). The clinical significance of the PRS derived from the MTAG analysis was validated in independent samples: first, in advanced glaucoma cases (ANZRAG and samples from Southampton/Liverpool in the UK), and second, in a prospectively monitored clinical cohort with early manifest glaucoma (PROGRESSA). b, Prediction in BMES, where we removed the IGGC VCDR and IGGC IOP GWAS from the training datasets, given that they contain BMES data. c, Prediction in the UKBB glaucoma and ICD-10 POAG cases. Here we removed all glaucoma cases and 3,000 controls with IOP/VCDR measurements as well as their relatives from UKBB VCDR/IOP GWAS. We also evaluated the performance of PRS in non-European ancestry (192 cases and 6,841 controls of South Asian ancestry in UKBB). d, Cumulative risk of glaucoma in UKBB. For the analysis of <i>MYOC</i> p.Gln368Ter carriers ($n = 965$; cases = 72; controls = 893), participants were stratified into tertiles of PRS. We also examined cumulative risk of glaucoma in the general population (<i>i.e.</i> in <i>MYOC</i> p.Gln368Ter non-carriers, $n = 381,196$; cases = 7,381; controls = 373,815) stratifying by deciles of the PRS. The discovery and testing datasets were designed to derive the PRS with no sample overlap (Supplementary Note).</p>

2

3

2. Supplementary Information:

4

A. Flat Files

Item	Present?	Filename This should be the name the file is saved as when it is uploaded to our system, and should include the file extension. The extension must be .pdf	A brief, numerical description of file contents. i.e.: <i>Supplementary Figures 1-4, Supplementary Note, and Supplementary Tables 1-4.</i>
Supplementary Information	Yes	NG_format_glaucoma_multitrait_SuppAppendix_merge	Supplementary Note, Supplementary Figures 1-13 and Supplementary Tables 1-13
Reporting Summary	Yes		

6

7

8

Multitrait analysis of glaucoma identifies new risk loci and enables polygenic prediction of disease susceptibility and progression

10

11

12

13

14

15

16

17

18

19

20

21

22

23

24

25

26

27

28

29

30

31

32

33

34

35

Jamie E. Craig^{1,40}, Xikun Han^{2,3,40*}, Ayub Qassim^{1,40}, Mark Hassall¹, Jessica N. Cooke Bailey⁴, Tyler G. Kinzy⁴, Anthony P. Khawaja⁵, Jiyuan An², Henry Marshall¹, Puya Gharahkhani², Robert P. Igo Jr.⁴, Stuart L. Graham⁶, Paul R. Healey^{7,8}, Jue-Sheng Ong², Tiger Zhou¹, Owen Siggs¹, Matthew H. Law², Emmanuelle Souzeau¹, Bronwyn Sheldrick¹, Pirro G. Hysi⁹, Kathryn P. Burdon¹⁰, Richard A. Mills¹, John Landers¹, Jonathan B. Ruddle¹¹, Ashish Agar¹², Anna Galanopoulos¹³, Andrew J. R. White⁷, Colin E. Willoughby^{14,15}, Nicholas Andrew¹, Stephen Best¹⁶, Andrea L. Vincent¹⁷, Ivan Goldberg¹⁸, Graham Radford-Smith², Nicholas G. Martin², Grant W. Montgomery¹⁹, Veronique Vitart²⁰, Rene Hoehn²¹, Robert Wojciechowski^{22,23}, Jost B. Jonas²⁴, Tin Aung²⁵, Louis R. Pasquale²⁶, Angela Jane Cree²⁷, Sobha Sivaprasad²⁸, Neeru A. Vallabh^{29,30}, NEIGHBORHOOD consortium³¹, UK Biobank Eye and Vision Consortium³¹, Ananth C. Viswanathan⁵, Francesca Pasutto³², Jonathan L. Haines⁴, Caroline C. W. Klaver³³, Cornelia M. van Duijn³⁴, Robert J. Casson³⁵, Paul J. Foster⁵, Peng Tee Khaw⁵, Christopher J. Hammond⁹, David A. Mackey^{10,36}, Paul Mitchell³⁷, Andrew J. Lotery³⁸, Janey L. Wiggs³⁹, Alex W. Hewitt^{10,40} and Stuart MacGregor^{2,40}

1. Department of Ophthalmology, Flinders University, Flinders Medical Centre, Bedford Park, Australia.

2. QIMR Berghofer Medical Research Institute, Brisbane, Australia.

3. School of Medicine, University of Queensland, Brisbane, Australia.

4. Department of Population and Quantitative Health Sciences, Institute for Computational Biology, Case Western Reserve University School of Medicine, Cleveland, OH, USA.

5. NIHR Biomedical Research Centre, Moorfields Eye Hospital NHS Foundation Trust and UCL Institute of Ophthalmology, London, UK.

6. Faculty of Medicine and Health Sciences, Macquarie University, Sydney, Australia.

7. Centre for Vision Research, Westmead Institute for Medical Research, University of Sydney,

- 36 Sydney, Australia.
- 37 8. Clinical Ophthalmology & Eye Health, Westmead Clinical School, University of Sydney,
38 Sydney, Australia.
- 39 9. Department of Ophthalmology, King's College London, St. Thomas' Hospital, London, UK.
- 40 10. Menzies Institute for Medical Research, University of Tasmania, Hobart, Australia.
- 41 11. Centre for Eye Research Australia, University of Melbourne, Melbourne, Australia.
- 42 12. Department of Ophthalmology, Prince of Wales Hospital, Randwick, New South Wales,
43 Australia.
- 44 13. South Australian Institute of Ophthalmology, Royal Adelaide Hospital, Adelaide, South
45 Australia, Australia.
- 46 14. Biomedical Sciences Research Institute, Ulster University, Coleraine, Northern Ireland, UK.
- 47 15. Royal Victoria Hospital, Belfast Health and Social Care Trust, Belfast, Northern Ireland, UK.
- 48 16. Eye Department, Greenlane Clinical Centre, Auckland District Health Board, Auckland, New
49 Zealand.
- 50 17. Department of Ophthalmology, University of Auckland, Auckland, New Zealand.
- 51 18. Discipline of Ophthalmology, University of Sydney, Sydney Eye Hospital, Sydney, Australia.
- 52 19. Institute for Molecular Bioscience, University of Queensland, Brisbane, Australia.
- 53 20. MRC Human Genetics Unit, MRC Institute of Genetics & Molecular Medicine, University of
54 Edinburgh, Edinburgh, UK.
- 55 21. Department of Ophthalmology, University Hospital Bern, Inselspital, University of Bern, Bern,
56 Switzerland.
- 57 22. Department of Epidemiology and Medicine, Johns Hopkins Bloomberg School of Public
58 Health, Baltimore, MD, USA.
- 59 23. Computational and Statistical Genomics Branch, National Human Genome Research
60 Institute, National Institutes of Health, Bethesda, MD, USA.
- 61 24. Department of Ophthalmology, Medical Faculty Mannheim of the Ruprecht-Karls-University of
62 Heidelberg, Mannheim, Germany.
- 63 25. Singapore Eye Research Institute, Singapore National Eye Centre, Singapore.
- 64 26. Icahn School of Medicine at Mount Sinai, New York, NY, USA.
- 65 27. Clinical and Experimental Sciences, Faculty of Medicine, University of Southampton,
66 Southampton, UK.
- 67 28. NIHR Moorfields Biomedical Research Centre, London, UK.
- 68 29. Department of Eye and Vision Science, Institute of Ageing and Chronic Disease, University of
69 Liverpool, Liverpool, UK.
- 70 30. St Paul's Eye Unit, Royal Liverpool University Hospital, Liverpool, UK.
- 71 31. The individual members of this consortium are listed in the Supplementary Note.
- 72 32. Institute of Human Genetics, Friedrich-Alexander-Universität Erlangen-Nürnberg, Erlangen,
73 Germany.
- 74 33. Department of Ophthalmology, Erasmus Medical Center, Rotterdam, The Netherlands.
- 75 34. Department of Epidemiology, Erasmus Medical Center, Rotterdam, The Netherlands.

76 35. South Australian Institute of Ophthalmology, University of Adelaide, Adelaide, South Australia,
77 Australia.

78 36. Lions Eye Institute, Centre for Vision Sciences, University of Western Australia, Nedlands,
79 Australia.

80 37. Department of Ophthalmology and Westmead Institute for Medical Research, University of
81 Sydney, Sydney, Australia.

82 38. Clinical and Experimental Sciences, Faculty of Medicine, University of Southampton,
83 Southampton, UK.

84 39. Department of Ophthalmology, Harvard Medical School, Massachusetts Eye and Ear
85 Infirmary, Boston, MA, USA.

86 40. These authors contributed equally.

87

88 *E-mail: Xikun.Han@qimrberghofer.edu.au

89

90 **Glaucoma, a disease characterized by progressive optic nerve degeneration, can be prevented**
91 **through timely diagnosis and treatment. We characterized optic nerve photographs of 67,040**
92 **UK Biobank participants and used a multitrait genetic model to identify risk loci for glaucoma.**
93 **A novel glaucoma polygenic risk score (PRS) enables effective risk stratification in unselected**
94 **glaucoma cases, and modifies penetrance of *MYOC* p.Gln368Ter, the most common glaucoma-**
95 **associated myocilin variant. In the unselected glaucoma population, individuals in the top PRS**
96 **decile reach an absolute risk for glaucoma 10 years earlier than the bottom decile, and are at**
97 **15-fold increased risk of developing advanced glaucoma (top 10% vs. remaining 90% OR =**
98 **4.20). The PRS predicts glaucoma progression in prospectively monitored early manifest**
99 **glaucoma cases ($P = 0.004$), and surgical intervention in advanced disease ($P = 3.6 \times 10^{-6}$). This**
100 **glaucoma PRS will facilitate the development of a personalized approach for earlier treatment**
101 **of high-risk individuals, with less intensive monitoring and treatment possible for lower-risk**
102 **groups.**

103

104 Glaucoma refers to a group of ocular conditions united by a clinically characteristic optic neuropathy
105 associated with, but not dependent on, elevated intraocular pressure¹. It is the leading cause of
106 irreversible blindness worldwide and is predicted to affect 76 million by 2020^{2,3}. There is no single
107 definitive biomarker for glaucoma, and diagnosis involves assessing clinical features, with
108 characterization of the optic nerve head carrying the strongest evidential weight. Primary open-angle
109 glaucoma (POAG) is the most prevalent subtype of glaucoma in people of European and African

110 ancestry^{2,4}. POAG is asymptomatic in the early stages, and currently approximately half of all cases in
111 the community are undiagnosed even in developed countries⁵. Early detection is paramount as
112 existing treatments are unable to restore vision that has been lost, and late presentation is a major
113 risk factor for blindness⁶. Thus, better strategies to identify high-risk individuals are urgently needed⁷,
114 and more refined approaches can capitalize on the fact that POAG is one of the most heritable of all
115 common human diseases⁸⁻¹⁰. The lack of a currently cost-effective screening strategy for glaucoma⁷,
116 coupled with very high heritability, make glaucoma an ideal candidate disease for the development
117 and application of a polygenic risk score to facilitate risk stratification.

118 Overlap of features shared by healthy optic nerves with those in early stages of glaucoma
119 makes it a difficult disease to diagnose early, necessitating costly ongoing monitoring of patients for
120 progressive optic nerve degeneration¹. Once a glaucoma diagnosis is established, rates of
121 progression vary widely between individuals, and considerable time can elapse before surveillance
122 techniques adequately differentiate slow from more rapidly progressing cases¹. Progressive vision
123 loss from glaucoma can be slowed, or in some cases halted, by timely intervention to reduce
124 intraocular pressure using medical therapy, laser trabeculoplasty or incisional surgery¹. The ability to
125 predict progression is currently crude, with delays in treatment escalation for high-risk individuals an
126 important and inevitable consequence, as well as substantial cost and morbidity associated with
127 overtreatment of lower risk cases.

128 The chronicity, heritability, clinical heterogeneity and treatability of POAG make it an ideal
129 candidate for genetic risk profiling^{11,12}. In this study, we evaluated the optic nerve head in 67,040 UK
130 Biobank participants (UKBB), enabling the largest genome-wide association study (GWAS) on optic
131 nerve morphology to date, using vertical cup-disc ratio (VCDR) as an endophenotype for glaucoma.
132 We then incorporated additional genetic data from a second well established glaucoma
133 endophenotype, intraocular pressure (IOP), and combined this with glaucoma disease status using a
134 recently developed multiple trait analysis of GWAS (MTAG)¹³ approach to first identify new risk loci for
135 glaucoma, and then generate a comprehensive glaucoma polygenic risk score (PRS). We examined
136 the impact of newly implicated glaucoma genes in independent case-control cohorts from Australia,
137 the United States, and the United Kingdom, and then evaluated the utility of the PRS for predicting
138 glaucoma risk, and important clinical outcomes in well-characterized cases across a range of disease
139 severities.

140

141 **Results**

142 **Study design.** Our overall study design is illustrated in Extended Data Figure 1a. We first conducted
143 a GWAS on glaucoma (7,947 cases and 119,318 controls) and on the key endophenotypes for
144 glaucoma: VCDR (including new data on 67,040 UKBB participants, and International Glaucoma
145 Genetics Consortium, IGGC, $n = 23,899$) and intraocular pressure (including data on 103,914 UKBB
146 participants and GWAS summary statistics from IGGC, $n = 29,578$; Supplementary Table 1). These
147 data were then combined using MTAG¹³ to identify new glaucoma risk loci and to construct a PRS.
148 The clinical significance of the PRS was investigated in advanced glaucoma cases in two populations,
149 and a separate prospectively monitored clinical cohort with early manifest glaucoma. The predictive
150 ability of the PRS was also explored in other datasets; however, to ensure our results generalize to
151 further cohorts, we selected mutually exclusive samples for inclusion in the discovery and testing
152 datasets to ensure no sample overlap. When required, we re-derived the PRS to ensure no sample
153 overlap (Extended Data Fig. 1b-d and Supplementary Note).

154

155 **Discovery of novel optic nerve morphology loci.** GWAS of VCDR (adjusted for vertical disc
156 diameter) identified 76 statistically independent, genome-wide significant SNPs (66 loci), of which 49
157 SNPs (43 loci) had not previously been associated with VCDR (Supplementary Figs. 1 and 2, and
158 Supplementary Table 2). Using LD score regression, we found no evidence for genomic inflation
159 (intercept = 1.04, s.e. = 0.01, Supplementary Fig. 3). The genetic correlation between VCDR
160 (adjusted for vertical disc diameter) and glaucoma in UKBB was 0.50 (s.e. = 0.05); the correlation in
161 effect size estimates at the 76 SNPs was 0.60 ($P = 9.0 \times 10^{-9}$, Supplementary Fig. 4). We further
162 combined UKBB VCDR (adjusted for vertical disc diameter) GWAS and IGGC VCDR GWAS
163 summary statistics using MTAG, and identified 107 independent genome-wide significant SNPs
164 (across 90 loci, Supplementary Table 3) for VCDR (adjusted for vertical disc diameter). As previously
165 reported, the genetic correlation between intraocular pressure and glaucoma was high (0.71)¹⁵, but as
166 expected the genetic correlation between VCDR (adjusted for vertical disc diameter) and intraocular
167 pressure was substantially lower (0.22, s.e. = 0.03).

168

169 **Discovery of novel glaucoma loci via multivariate analysis.** Given the high correlation between
170 glaucoma and its endophenotypes, we then conducted a multivariate GWAS (with 8,002,429 SNPs
171 after quality control) to identify 114 statistically independent SNPs (107 loci, $P < 5 \times 10^{-8}$) associated
172 with glaucoma; this includes all previously published glaucoma loci as well as 49 novel loci (Fig. 1,
173 Supplementary Figs. 5 and 6, and Supplementary Table 4). At the more stringent multiple testing
174 threshold ($P < 1 \times 10^{-8}$) suggested by a simulation study¹⁶, 95 loci reach significance, 39 of which are
175 novel (Supplementary Table 4); 27 of the 49 top SNPs at these novel loci were not associated
176 individually with any of the individual input traits at the genome-wide significance level ($P = 5 \times 10^{-8}$)
177 and were only found to reach this threshold for glaucoma due to the MTAG method leveraging the
178 strong correlation between the input traits. We then attempted to replicate the 49 novel SNPs in two
179 independent glaucoma cohorts (ANZRAG and NEIGHBORHOOD). Given the much smaller effective
180 sample size of these replication cohorts (versus the discovery datasets from the MTAG analysis), we
181 did not expect all of the SNPs to be strongly associated; rather, if they were genuine associations, we
182 would expect the ORs to be highly concordant, with some of the smaller ORs being individually non-
183 significant. The concordance between the discovery cohort and our replication cohorts log ORs was
184 excellent (correlation 0.88, $P = 1.6 \times 10^{-36}$), indicating that our multivariate model was successful in
185 identifying genuine glaucoma risk loci (Fig. 2 and Supplementary Fig. 7). Of the 49 novel SNPs, nine
186 were replicated after Bonferroni correction ($P < 0.05/49 = 0.001$, one-sided test, bold text in
187 Supplementary Table 4), 26 were associated at a nominal significance level ($P < 0.05$, one-sided test,
188 italic text in Supplementary Table 4), and 46 (94%) were in the expected direction. While the
189 concordance between the multivariate and the glaucoma replication sample log ORs was high, only
190 nine of the 49 loci were significant for glaucoma after correction for multiple comparisons, and further
191 studies are required to replicate the remaining 40 loci for glaucoma.

192 We conducted a genome-wide gene-based association analysis and a gene set enrichment
193 analysis to assess which predefined biological pathways were enriched in our multitrait glaucoma
194 GWAS; we found 196 genes and 14 gene sets, respectively, that were significant after Bonferroni
195 correction (Supplementary Tables 5 and 6). The most significant pathways were also previously
196 implicated (i.e. extracellular matrix, collagen, and circulatory system development)^{15,17}. Further studies
197 are warranted to investigate the role of these pathways in the risk of glaucoma.

198

199 **Optimizing prediction of glaucoma risk by combining correlated traits.** We derived our PRS
200 based on the MTAG of GWAS data from glaucoma and its endophenotypes. As well as increasing the
201 number of SNPs that reach genome-wide significance (mean chi-squared statistic increased from
202 1.12 to 1.30, implying our effective sample size was 2.59 times larger than if we had used UKBB
203 glaucoma cases and controls alone), our multivariate model improved the power of risk prediction by
204 reducing the error in the estimate of the effect size for every SNP (assuming the MTAG homogeneity
205 assumption is true, see Discussion)¹³. We first tested the discriminatory power of the MTAG-derived
206 PRS in the ANZRAG cohort of advanced glaucoma. We found SNPs with MTAG *P* values ≤ 0.001
207 (corresponding to 2,673 uncorrelated SNPs after LD-clumping at $r^2 = 0.1$ and *P*-value threshold at
208 0.001) had the highest Nagelkerke R^2 (13.2%) and AUC (0.68, 95%CI: 0.67-0.70) (Supplementary
209 Table 7). The MTAG PRS has better prediction ability than any of the input traits alone
210 (Supplementary Table 8). Based on this, we set the *P*-value threshold at 0.001 for all the remaining
211 prediction target sets (PROGRESSA, BMES, UKBB).

212 The MTAG-derived PRS was effective at separating advanced glaucoma individuals in terms
213 of risk, with a clear dose-response over deciles (Fig. 3a and Supplementary Fig. 8). In ANZRAG,
214 individuals in the top decile of the PRS had 14.9-fold higher risk (95%CI: 10.7-20.9) relative to the
215 bottom decile, with even better discrimination for the more common high-tension glaucoma (OR =
216 21.5, 95%CI: 12.5-37.0) than normal-tension glaucoma (Supplementary Fig. 9). We replicated the
217 dose-response of the PRS in a smaller UK advanced glaucoma dataset (Southampton and Liverpool);
218 the top versus bottom PRS decile had OR = 11.6 (95%CI: 6.0-25.3), with again better discrimination
219 for high-tension glaucoma (OR = 12.9, 95%CI: 6.2-31.3). While comparing the top and bottom deciles
220 shows the dose-response across deciles, one can also consider the risk in the high PRS individuals
221 versus all others; when this is done in ANZRAG, the OR is 4.2 and 8.5 in the top 10% and 1%,
222 respectively, of individuals versus all remaining individuals (Supplementary Table 9).

223

224 **Glaucoma risk score performance in individuals carrying high penetrance variants.** Previous
225 studies indicated that PRS modifies the penetrance of rare *BRCA1/2* mutation carriers for breast,
226 ovarian, and prostate cancers^{18,19}. Although the MTAG-derived PRS only contains common variants,
227 given it indexes general glaucoma risk, we hypothesized that it could stratify individuals carrying
228 known high-penetrance glaucoma variants. Pathogenic *MYOC* (Myocilin) gene variants account for 2-

229 4% of POAG cases among most populations, the most common disease-causing variant being
230 p.Gln368Ter (rs74315329)²⁰. Penetrance is age-related and is lower in population-based than family-
231 based studies^{20,21}. We speculated that this difference in penetrance could be due to enrichment of
232 common glaucoma-associated variants in families modifying age-related penetrance. Within UKBB,
233 we identified 965 *MYOC* p.Gln368Ter carriers based on imputation (Supplementary Note)²². Figure 3c
234 shows the cumulative risk of glaucoma in p.Gln368Ter carriers, stratifying by PRS tertiles. For
235 p.Gln368Ter carriers in the lowest tertile PRS, glaucoma risk remained very low (2%) up to age 60. In
236 contrast, the highest tertile PRS group had substantially increased risk of early diagnosis, reaching a
237 6-fold increase in absolute risk of glaucoma by age 60, relative to the lowest PRS tertile (considering
238 whole age range, hazard ratio = 3.4, 95%CI: 1.7-6.6). This supports the utility of PRS in optimizing
239 risk stratification and prediction, and early screening for patients carrying high penetrance *MYOC*
240 variants in the presence of high PRS scores.

241

242 **Potential for glaucoma risk score in screening in the general population.** We considered a
243 general population screening scenario using UKBB (PRS was re-derived to ensure no sample
244 overlap; Extended Data Fig. 1d), where we excluded the 965 *MYOC* p.Gln368Ter carriers. Over the
245 40-69 year old age range for individuals sampled in UKBB, glaucoma prevalence increases from
246 0.1% at age 40, reaching 3% (95%CI: 2.9-3.1%) by age 64. The MTAG-derived PRS stratifies UKBB
247 participants very effectively; for those in the top PRS decile, 3% prevalence (prevalence in general
248 population) is reached by age 59, while it takes an additional 10 years for this disease prevalence to
249 be reached for people in the bottom PRS decile. Alternatively, the prevalence can be well stratified by
250 PRS deciles (Fig. 3d).

251 To benchmark the performance of the MTAG-derived PRS with traditional risk factors, we
252 computed the AUC in datasets for which this was possible: BMES, UKBB glaucoma (broad glaucoma
253 definition), and UKBB POAG (ICD-10 definition) (Fig. 3b, Supplementary Table 11 (PRS was re-
254 derived to ensure no sample overlap), and Extended Data Fig. 1). In the BMES, our PRS provided
255 additional predictive ability beyond that imparted by traditional risk factors (age, sex, and self-reported
256 family history (FH)), with a significant change in the AUC (from 0.73 to 0.80, $P = 0.002$, Fig. 3b). Clear
257 improvement in prediction using this PRS is also observed in people of South Asian ancestry
258 (Supplementary Table 11), though we were underpowered to explore this further across other groups.

259 A previous study examined the cost-effectiveness requirements for glaucoma screening and
260 highlighted the key age 50-60 bracket⁷. In the BMES data (Extended Data Fig. 1b), screening only
261 those with a top decile PRS identified 40% of all early onset cases in age 50-60 bracket (40% of the
262 10 cases, $P = 0.013$). Such individuals represent a set of individuals likely to benefit from referral for
263 immediate clinical assessment—with skilled clinical examination, retinal imaging, and visual fields. We
264 replicated this result in the UKBB POAG cohort (ICD10 cases in Extended Data Fig. 1c, top 10% PRS
265 screening finds 29% of 24 cases aged 50-60, $P = 0.0075$). In this way, PRS-based screening would
266 satisfy the cost-effectiveness requirements of Burr *et al.*⁷, identify a meaningful proportion of cases,
267 and capture those cases most at risk of severe disease.

268

269 **Clinical implications of the glaucoma risk score.** We evaluated the predictive power of the PRS in
270 advanced glaucoma; in 1,336 ANZRAG advanced POAG cases with accurate age at diagnosis
271 information available (Supplementary Table 12), the PRS was significantly associated with age at
272 diagnosis of POAG ($P = 1.8 \times 10^{-5}$). Individuals in the top 10% of the PRS distribution were on
273 average diagnosed 7 years younger than people in the bottom 10% (Fig. 4a). We also found
274 ANZRAG individuals with higher PRS had more family members affected by glaucoma ($P = 3.5 \times 10^{-9}$),
275 with the highest decile having twice as many members affected (Supplementary Fig. 10).

276 Retinal nerve fibre layer thinning is a major structural change evident in early stage
277 glaucoma²³. In the early manifest glaucoma (PROGRESSA) cohort, the PRS predicted both the
278 proportion lost and rate of loss of peripapillary retinal nerve fibre layer. Given that glaucomatous loss
279 of retinal ganglion cells generally progresses unequally between eyes, with some quadrants of the
280 retina damaged more rapidly than others, we analyzed the most affected quadrant of the most
281 affected eye in individuals with early manifest glaucoma and greater than two years of longitudinal
282 optical coherence tomography data. The PRS was significantly associated with the proportion of
283 retinal nerve fibre layer lost from baseline to most recent review, even after adjustment for known risk
284 factors: age, intraocular pressure and retinal nerve fibre layer thickness at presentation ($P = 0.004$;
285 Fig. 4b and Supplementary Table 13). Expressed in terms of rate of loss, each decile change in PRS
286 was associated with an accelerated progression rate of 0.05 $\mu\text{m}/\text{year}$, which was twice the rate of
287 thinning per mmHg (approximately 1 decile change for intraocular pressure) of baseline intraocular
288 pressure (0.022 $\mu\text{m}/\text{year}$).

289 Incisional surgery for glaucoma (trabeculectomy) is highly effective at reducing intraocular
290 pressure, but has significant complications which can adversely impact vision¹. Trabeculectomy is
291 performed either when intraocular pressure is unable to be controlled with medical or laser therapy, or
292 when there is progressive visual field loss despite well controlled intraocular pressure. Patients with a
293 high PRS were more likely to have undergone surgery for glaucoma (Fig. 4c and Supplementary
294 Figure 11). In the ANZRAG cohort of POAG cases, a higher PRS was associated with requiring
295 trabeculectomy, even after adjustment for maximum recorded intraocular pressure and age ($P = 3.6 \times$
296 10^{-6}), the OR of requiring trabeculectomy in either eye for people in the top PRS decile was 1.78
297 (95%CI: 1.07–3.00) compared to the bottom decile. We observed a very similar trend in our UK
298 replication (Southampton/Liverpool) samples (Supplementary Fig. 11).

299

300 **Discussion**

301 Through a large-scale multivariate GWAS we identified novel genes for glaucoma, the leading cause
302 of irreversible blindness worldwide². Despite a smaller replication cohort, many of these novel hits
303 were replicated, and all but three SNPs showed a consistent direction of effect. We then expanded
304 this analysis to derive a PRS and interrogated its utility across a wide spectrum of clinically relevant
305 glaucoma outcomes.

306 From the multivariate GWAS, we identified 49 novel loci associated with glaucoma (nine of
307 which replicated after correction for multiple comparisons in independent glaucoma case-control
308 cohorts; 26 were replicated with $P < 0.05$). Interestingly, most of the loci replicated at $P < 0.001$ are at
309 genes previously associated with glaucoma risk factors (myopia, CCT, IOP, VCDR). Specifically,
310 *RSPO1* is associated with ocular axial length²⁴. *BICC1* is associated with myopia and corneal
311 astigmatism^{25,26,27}. *POU6F2* modulates corneal thickness and increases glaucoma risk in animal
312 experiments²⁸. *FBXO32*, *PTPN1*, and *VPS13C* are associated with IOP^{15,29,30}, while *CASC20* was
313 identified in our VCDR (adjusted for vertical disc diameter) GWAS. These findings show that our
314 multivariate GWAS improves power to identify novel glaucoma genes and advance our understanding
315 of the causes of glaucoma risk.

316 The MTAG-derived PRS was validated in independent samples, confirming its high predictive
317 ability. Individuals in the top PRS decile were at 15-fold increased risk of advanced glaucoma, and at

318 21.5-fold increased risk of advanced high tension glaucoma, relative to the bottom decile, which
319 represents a substantial improvement on previously reported genetic profiling strategies (where,
320 based on SNPs that were genome-wide significantly associated with intraocular pressure and SNPs
321 previously associated with VCDR and glaucoma, top decile individuals had a 5.6-fold increased
322 risk)¹⁵. This new glaucoma PRS also outperforms those derived from other well-studied conditions; for
323 example, our OR comparing the top 1% PRS individuals versus the remaining individuals was 8.5,
324 which is higher than that seen in a recent study which surveyed coronary artery, atrial fibrillation, type
325 2 diabetes, inflammatory bowel disease and breast cancer³¹. The etiology of complex diseases
326 depends on both environmental and genetic factors; thus, PRS alone will never achieve the very high
327 predictive power (e.g. AUC > 0.99) required for accurate population screening³². Our glaucoma PRS
328 will be primarily useful for stratifying individuals into risk groups; for example in the BMES data,
329 screening the top decile of the PRS in individuals between 50-60 years old identifies 40% of cases.
330 Moreover, as argued by Khera *et al.*³¹, individuals with a high PRS for glaucoma are likely to be at a
331 similar risk to individuals carrying rare “high penetrance” *MYOC* mutations²¹. Finally, the PRS
332 performance for glaucoma is particularly noteworthy given the clinical implications of identifying at-risk
333 individuals and the prevention of irreversible blindness with readily available treatment proven to be
334 effective at preventing visual loss.

335 While current treatments are effective in preventing or reducing POAG progression¹², many
336 patients are not diagnosed before irreversible damage to visual function has already occurred. Earlier
337 diagnosis of glaucoma can reduce glaucoma blindness, and our work demonstrates that people with a
338 higher PRS require earlier clinical assessment. In the UKBB, individuals in the top PRS decile reach
339 an equivalent absolute risk for glaucoma 10 years earlier than people in the bottom decile. In
340 advanced glaucoma cases, individuals in the top decile were diagnosed 7 years earlier than those in
341 the bottom decile. Similarly, the MTAG-derived PRS was associated with significantly earlier disease
342 onset in UK Biobank *MYOC* p.Gln368Ter carriers who are at high disease risk. The MTAG-derived
343 PRS can also identify people with early manifest glaucoma who are at higher probability of disease
344 progression, as well as the likelihood of requiring surgical intervention, which is highly effective at
345 reducing intraocular pressure, but carries substantial treatment morbidity meaning it should always be
346 targeted specifically to those at higher risk of disease progression and blindness.

347 A concern with the MTAG method is the homogeneous assumption, which could be violated
348 for some SNPs that have no effect on one trait but are non-null for other traits (*i.e.* it is possible that a
349 small number of the variants may be more specific for IOP or VCDR rather than glaucoma). The
350 homogeneity assumption has been studied in detail by Turley *et al.*¹³ We have evaluated the possible
351 inflation using max False Discovery Rate (maxFDR) as recommended¹³. The baseline maxFDR for
352 MTAG glaucoma-specific input GWAS summary statistics is 0.049, and the maxFDR for MTAG
353 glaucoma-specific output summary statistics is 0.03. As these are similar, there is no evidence of
354 inflation due to violation of the homogeneity assumption. As recommended by the MTAG authors, we
355 also performed replication analysis to assess the credibility of novel SNPs in two independent data
356 sets (an Australasian cohort of advanced glaucoma (ANZRAG) and a consortium of cohorts from the
357 United States (NEIGHBORHOOD)); this analysis shows there is very good concordance between the
358 MTAG-based effect sizes and those from the glaucoma cohorts. Furthermore, using MTAG output
359 instead of the individual input traits improves the predictions in independent cohorts (Supplementary
360 Table 8), providing additional evidence that we are not merely identifying IOP- or VCDR-specific loci
361 that have no effect on glaucoma. Further research needs to be undertaken to investigate the
362 biological mechanisms of these novel genes on glaucoma risk.

363 A limitation of this work, is that in our 7,947 UKBB glaucoma cases, only a small proportion
364 had documented disease subtype; however, since the proportion of UK glaucoma cases that have
365 POAG is high (87% in a recent study⁴), this is unlikely to have a large influence on our results. A
366 further limitation is that it is not yet clear how applicable our findings are to other populations. We
367 showed that the PRS improved prediction accuracy over and above traditional risk factors in
368 homogeneous groups (as defined by genetic principal components) of either European or South
369 Asian ancestry. The performance of the PRS in other populations should be tested to investigate the
370 generalizability of our findings. The performance of the PRS in aiding clinical decision making and
371 guiding earlier treatment could be evaluated prospectively in a longitudinal intervention study, with
372 participants randomized to have their PRS provided or withheld from their treating specialist.

373 In summary, we have applied a multivariate approach using weighted data on glaucoma, and
374 endophenotypes intraocular pressure and VCDR, to identify novel glaucoma loci, and develop a
375 polygenic risk score. This PRS was shown to be predictive of: 1) increasing risk of advanced
376 glaucoma; 2) glaucoma status significantly beyond traditional risk factors; 3) earlier age of glaucoma

377 diagnosis; 4) high levels of absolute risk in persons carrying high penetrance glaucoma variants; 5)
378 increasing likelihood of disease progression in early stage disease, and 6) increasing likelihood of
379 incisional glaucoma surgery in advanced disease. This glaucoma PRS has good predictive power
380 across a range of clinical cohorts and its application will facilitate the rational allocation of resources
381 through clinical screening and timely treatment in high-risk patients, with reduced clinical monitoring
382 costs in lower risk groups.

383

384

385 **Acknowledgements**

386 This work was conducted using the UK Biobank Resource (application number 25331) and publicly
387 available data from the International Glaucoma Genetics Consortium. The UK Biobank was
388 established by the Wellcome Trust medical charity, Medical Research Council (UK), Department of
389 Health (UK), Scottish Government, and Northwest Regional Development Agency. It also had funding
390 from the Welsh Assembly Government, British Heart Foundation, and Diabetes UK. The eye and
391 vision dataset has been developed with additional funding from The NIHR Biomedical Research
392 Centre at Moorfields Eye Hospital and the UCL Institute of Ophthalmology, Fight for Sight charity
393 (UK), Moorfields Eye Charity (UK), The Macula Society (UK), The International Glaucoma Association
394 (UK) and Alcon Research Institute (USA). This work was also supported by grants from the National
395 Health and Medical Research Council (NHMRC) of Australia (#1107098; 1116360, 1116495,
396 1023911), the Ophthalmic Research Institute of Australia, the BrightFocus Foundation, UK and Eire
397 Glaucoma Society and Charitable Funds from Royal Liverpool University Hospital. S.M., J.E.C.,
398 K.P.B., and A.W.H. are supported by NHMRC Fellowships. S.M. was supported by an Australian
399 Research Council Future Fellowship. L.R.P. is supported by NIH R01 EY015473. X.H. is supported by
400 the University of Queensland Research Training Scholarship and QIMR Berghofer PhD Top Up
401 Scholarship. We thank David Whiteman, Rachel Neale and Catherine Olson for providing access to
402 QSKIN samples for use as controls as part of NHMRC Grant 1063061. We thank Scott Wood, John
403 Pearson and Scott Gordon from QIMR Berghofer for support. The NEIGHBORHOOD consortium is
404 supported by NIH grants P30 EY014104, R01 EY015473 and R01 EY022305.

405

406 **Author contributions**

407 S.M., A.W.H., J.E.C., P.G., J.L.W., and D.A.M. designed the study and obtained funding. X.H., A.Q.,
408 M.H., J.N.C.B., T.G.K., A.P.K., P.G.H., J.A., H.M., P.G., R.P.I., J.-S.O., T.Z., O.S., M.H.L., and S.M.
409 analyzed the data. J.E.C., X.H., A.Q., M.H., A.P.K., H.M., R.P.I., S.L.G., P.R.R., O.S., E.S., B.S.,
410 P.G.H., K.P.B., R.A.M., J.L., J.B.R., A.A., A.G., A.J.R.W., C.E.W., N.A., S.B., A.L.V., I.G., G.R.-S.,
411 N.G.M., G.W.M., V.V., R.H., R.W., J.B.J., T.A., L.R.P., A.J.C., S.S., N.A.V., A.C.V., F.P., J.L.H.,
412 C.C.W.K., C.M.v.D., R.J.C., P.J.F., P.T.K., C.J.H., D.A.M., P.M., A.J.L., J.L.W., A.W.H., and S.M.
413 contributed to data collection and contributed to genotyping. X.H., J.E.C., A.Q., A.W.H., and S.M.
414 wrote the first draft of the paper. All authors contributed to the final version of the paper.

415

416

417 **Competing interests**

418 D.A.M. is consultant/advisor to Allergan, Inc. J.E.C., A.W.H. and S.M. are listed as co-inventors on a
419 patent application for the use of genetic risk scores to determine risk and guide treatment.

420

421

422

423 **References:**

- 424 1. Weinreb, R. N. & Khaw, P. T. Primary open-angle glaucoma. *Lancet* **363**, 1711–1720 (2004).
- 425 2. Tham, Y.-C. *et al.* Global prevalence of glaucoma and projections of glaucoma burden
426 through 2040: a systematic review and meta-analysis. *Ophthalmology* **121**, 2081–2090 (2014).
- 427 3. Quigley, H. A. & Broman, A. T. The number of people with glaucoma worldwide in 2010 and
428 2020. *Br. J. Ophthalmol.* **90**, 262–267 (2006).
- 429 4. Chan, M. P. Y. *et al.* Glaucoma and intraocular pressure in EPIC-Norfolk Eye Study: cross
430 sectional study. *BMJ* **358**, j3889 (2017).
- 431 5. Mitchell, P., Smith, W., Attebo, K. & Healey, P. R. Prevalence of open-angle glaucoma in
432 Australia. The Blue Mountains Eye Study. *Ophthalmology* **103**, 1661–1669 (1996).
- 433 6. Fraser, S., Bunce, C. & Wormald, R. Risk factors for late presentation in chronic glaucoma.
434 *Invest. Ophthalmol. Vis. Sci.* **40**, 2251–2257 (1999).
- 435 7. Burr, J. M. *et al.* The clinical effectiveness and cost-effectiveness of screening for open angle
436 glaucoma: a systematic review and economic evaluation. *Health Technol. Assess.* **11**, iii–iv, ix–x,
437 1–190 (2007).
- 438 8. Wang, K., Gaitsch, H., Poon, H., Cox, N. J. & Rzhetsky, A. Classification of common human
439 diseases derived from shared genetic and environmental determinants. *Nat. Genet.* **49**, 1319–
440 1325 (2017).
- 441 9. Sanfilippo, P. G., Hewitt, A. W., Hammond, C. J. & Mackey, D. A. The heritability of ocular
442 traits. *Surv. Ophthalmol.* **55**, 561–583 (2010).
- 443 10. Choquet, H. *et al.* A multiethnic genome-wide association study of primary open-angle
444 glaucoma identifies novel risk loci. *Nat. Commun.* **9**, 2278 (2018).
- 445 11. Leske, M. C., Heijl, A., Hyman, L., Bengtsson, B. & Komaroff, E. Factors for progression and
446 glaucoma treatment: the Early Manifest Glaucoma Trial. *Curr. Opin. Ophthalmol.* **15**, 102–106
447 (2004).
- 448 12. Garway-Heath, D. F. *et al.* Latanoprost for open-angle glaucoma (UKGTS): a randomised,
449 multicentre, placebo-controlled trial. *Lancet* **385**, 1295–1304 (2015).
- 450 13. Turley, P. *et al.* Multi-trait analysis of genome-wide association summary statistics using
451 MTAG. *Nat. Genet.* **50**, 229–237 (2018).
- 452 14. Bengtsson, B. The variation and covariation of cup and disc diameters. *Acta Ophthalmol.* **54**,

453 804–818 (1976).

454 15. MacGregor, S. *et al.* Genome-wide association study of intraocular pressure uncovers new
455 pathways to glaucoma. *Nat. Genet.* **50**, 1067–1071 (2018).

456 16. Wu, Y., Zheng, Z., Visscher, P. M. & Yang, J. Quantifying the mapping precision of genome-
457 wide association studies using whole-genome sequencing data. *Genome Biol.* **18**, 86 (2017).

458 17. Huang, L. *et al.* Genome-wide analysis identified 17 new loci influencing intraocular pressure
459 in Chinese population. *Sci. China Life Sci.* **62**, 153–164 (2019).

460 18. Kuchenbaecker, K. B. *et al.* Evaluation of polygenic risk scores for breast and ovarian cancer
461 risk prediction in *BRCA1* and *BRCA2* mutation carriers. *J. Natl. Cancer Inst.* **109**, (2017).

462 19. Lecarpentier, J. *et al.* Prediction of breast and prostate cancer risks in male *BRCA1* and
463 *BRCA2* mutation carriers using polygenic risk scores. *J. Clin. Oncol.* **35**, 2240–2250 (2017).

464 20. Hewitt, A. W., Mackey, D. A. & Craig, J. E. Myocilin allele-specific glaucoma phenotype
465 database. *Hum. Mutat.* **29**, 207–211 (2008).

466 21. Han, X. *et al.* Myocilin gene Gln368Ter variant penetrance and association with glaucoma in
467 population-based and registry-based studies. *JAMA Ophthalmol.* **137**, 28–35 (2019).

468 22. Gharahkhani, P. *et al.* Accurate imputation-based screening of Gln368Ter Myocilin variant in
469 primary open-angle glaucoma. *Invest. Ophthalmol. Vis. Sci.* **56**, 5087–5093 (2015).

470 23. Na, J. H. *et al.* Detection of glaucoma progression by assessment of segmented macular
471 thickness data obtained using spectral domain optical coherence tomography. *Invest.*
472 *Ophthalmol. Vis. Sci.* **53**, 3817–3826 (2012).

473 24. Cheng, C.-Y. *et al.* Nine loci for ocular axial length identified through genome-wide
474 association studies, including shared loci with refractive error. *Am. J. Hum. Genet.* **93**, 264–277
475 (2013).

476 25. Pickrell, J. K. *et al.* Detection and interpretation of shared genetic influences on 42 human
477 traits. *Nat. Genet.* **48**, 709–717 (2016).

478 26. Verhoeven, V. J. M. *et al.* Genome-wide meta-analyses of multiancestry cohorts identify
479 multiple new susceptibility loci for refractive error and myopia. *Nat. Genet.* **45**, 314–318 (2013).

480 27. Lopes, M. C. *et al.* Identification of a candidate gene for astigmatism. *Invest. Ophthalmol. Vis.*
481 *Sci.* **54**, 1260–1267 (2013).

482 28. King, R. *et al.* Genomic locus modulating corneal thickness in the mouse identifies POU6F2

483 as a potential risk of developing glaucoma. *PLoS Genet.* **14**, e1007145 (2018).
484 29. Khawaja, A. P. *et al.* Genome-wide analyses identify 68 new loci associated with intraocular
485 pressure and improve risk prediction for primary open-angle glaucoma. *Nat. Genet.* **50**, 778–782
486 (2018).
487 30. Gao, X. R., Huang, H., Nannini, D. R., Fan, F. & Kim, H. Genome-wide association analyses
488 identify new loci influencing intraocular pressure. *Hum. Mol. Genet.* **27**, 2205–2213 (2018).
489 31. Khera, A. V. *et al.* Genome-wide polygenic scores for common diseases identify individuals
490 with risk equivalent to monogenic mutations. *Nat. Genet.* **50**, 1219–1224 (2018).
491 32. Dudbridge, F. Power and predictive accuracy of polygenic risk scores. *PLoS Genet.* **9**,
492 e1003348 (2013).

493 **Figure Legends:**

494 **Figure 1 | Manhattan plot displaying glaucoma-specific *P* values from the multi-trait GWAS**

495 **(MTAG) analysis.** The samples used in multi-trait analysis is presented in Extended Data Figure 1a. Novel
496 SNPs are highlighted in red dots, with the nearest gene names in black text. Known SNPs are highlighted in
497 purple dots, with the nearest gene names in purple text. The red line is the genome-wide significance level at $5 \times$
498 10^{-8} .

499

500 **Figure 2 | Comparison of the effect sizes (log odds ratio) for 114 genome-wide significant**
501 **independent SNPs identified from the glaucoma multiple trait analysis of GWAS in the UKBB**
502 **versus those in independent glaucoma cohorts (meta-analysis of ANZRAG and**

503 **NEIGHBORHOOD).** Pearson's correlation coefficient is 0.88 ($P = 1.6 \times 10^{-36}$). The red line is the best fit line,
504 with the 95% confidence interval region in grey. Novel glaucoma SNPs are highlighted in red and known SNPs in
505 purple.

506

507 **Figure 3 | Multiple trait analysis of GWAS PRS prediction. a,** Odds ratio (OR) of developing advanced
508 glaucoma in the ANZRAG cohort (with 1,734 advanced glaucoma cases and 2,938 controls) for each PRS decile.
509 The square dots are the OR values (adjusted for sex and the first four principal components) and the error bars
510 are 95% confidence interval. The dashed line is the reference at the bottom PRS decile (OR = 1). **b,** AUCs of
511 PRS in BMES. The MTAG-derived PRS provided additional predictive ability on top of traditional risk factors (age,
512 sex, and self-reported family history (FH), DeLong's test $P = 0.002$). The AUC is based on a logistic regression
513 model with the coefficients for age, sex, FH and PRS estimated from the BMES data (Supplementary Table 10).
514 **c,** Cumulative risk of glaucoma in UKBB *MYOC* p.Gln368Ter carriers stratifying by the PRS (adjusted for sex and
515 first six genetic principal components). Here the cumulative risk of tertiles (with 95% confidence intervals) of PRS
516 are displayed given the relatively small number of *MYOC* p.Gln368Ter carriers ($n = 965$). **d,** Cumulative risk of
517 glaucoma for people in the top and bottom decile (with 95% confidence intervals) of PRS of the UKBB who do not
518 have the *MYOC* p.Gln368Ter variant (adjusted for sex and first six genetic principal components). The dashed
519 line is the reference line of cumulative risk at 3%.

520

521 **Figure 4 | Clinical implications of the glaucoma PRS. a,** Mean age at diagnosis (years) for each decile
522 of PRS in the ANZRAG cohort (linear regression $P = 1.8 \times 10^{-5}$). A total of 1,336 cases had accurate age at
523 diagnosis information. We calculated the mean age at diagnosis for each decile of PRS, adjusted for sex and the
524 first four principal components in a linear regression model. The square dots are the regression-based mean age
525 at diagnosis, with error bars for 95% confidence intervals. The red line is the line of best fit, with 95% confidence
526 intervals in grey. **b,** Proportion of preserved baseline retinal nerve fibre layer for PROGRESSA participants with
527 early manifest glaucoma plotted against PRS decile ($n = 388$; linear regression $P = 0.004$). The square dots are
528 the retinal nerve fibre layer proportions, with error bars showing 95% confidence intervals. The remaining retinal
529 nerve fibre layer proportion is calculated for the most affected quadrant of the most affected eye of each patient
530 — as determined on optical coherence tomography scans at baseline and latest follow-up scan. **c,** Proportion of
531 patients requiring trabeculectomy in either eye in the ANZRAG POAG cohort (linear regression $P = 3.6 \times 10^{-6}$).
532 There were 1,360 cases with records of surgical treatment status. The square dots represent the observed
533 average proportion of cases in each decile of PRS who required trabeculectomy, with 95% confidence interval
534 bars. The line of best fit is shown in red, with 95% confidence interval shaded in grey.

535

536 **Methods**

537 **Study design and overview.** Our overall study design is illustrated in Extended Data Figure 1. We
538 first conducted a GWAS on glaucoma and on the key endophenotypes for glaucoma: VCDR and
539 intraocular pressure. These data were then combined using MTAG¹³, a method for combining multiple
540 genetically correlated traits to maximize power for identifying new loci and improving genetic risk
541 prediction. Specifically, our MTAG analysis outputs *glaucoma-specific effect size estimates* and *P*-
542 values for single nucleotide polymorphisms (SNPs) across the genome. Newly associated loci ($P < 5$
543 $\times 10^{-8}$) were validated in two independent cohorts with well-characterised POAG. We created a PRS
544 based on the MTAG GWAS summary statistics. The clinical significance of the PRS was investigated
545 in advanced glaucoma cases in two populations, and a separate prospectively monitored clinical
546 cohort with early manifest glaucoma. The predictive ability of the PRS was also explored in other
547 datasets; however, to ensure our results generalize to further cohorts, we selected mutually exclusive
548 samples for inclusion in the discovery and testing datasets to ensure no sample overlap. When
549 required, we re-derived the PRS to avoid any sample overlap (Extended Data Fig. 1). Study
550 procedures were performed in accordance with the World Medical Association Declaration of Helsinki
551 ethical principles for medical research.

552

553 **Study populations.** Detailed information of individual studies, phenotypic definitions, and genetic
554 quality control procedures are provided in the Supplementary Note.

555 The UK Biobank (UKBB) is a population-based study of half a million people living in the
556 United Kingdom³³. We measured VCDR and vertical disc diameter in all subjects with gradable retinal
557 images (67,040 participants following exclusions, detailed in Supplementary Note) and undertook a
558 GWAS to identify SNPs influencing optic nerve head morphology. Vertical disc diameter adjustment of
559 the VCDR was used to account for optic cup and disc size covariation^{14,34}. To improve power in the
560 multi-trait analysis, we combined the VCDR data with data on corneal-compensated intraocular
561 pressure (103,914 participants) and glaucoma (7,947 cases, 119,318 controls) in the MTAG
562 analysis¹⁵. We also used publicly available VCDR and intraocular pressure GWAS summary results
563 for individuals of European descent from the International Glaucoma Genetics Consortium (IGGC;
564 $n_{\text{VCDR}} = 23,899$, $n_{\text{intraocular pressure}} = 29,578$)³⁵.

565 The Australian & New Zealand Registry of Advanced Glaucoma (ANZRAG) comprises 3,071
566 POAG cases of European descent, who were compared to 6,750 controls^{36,37}. For sub-analyses
567 restricted to advanced POAG, there were 1,734 advanced POAG cases and 2,938 controls, and of
568 these cases 1,336 participants had accurate age at diagnosis information available. Replication of the
569 ANZRAG findings was performed using 332 advanced glaucoma cases from Southampton and
570 Liverpool in the United Kingdom; for case-control analysis, cases were matched to 3,000 randomly
571 selected European ancestry individuals from the QSkin Sun and Health study³⁸. The National Eye
572 Institute Glaucoma Human Genetics Collaboration Heritable Overall Operational Database
573 (NEIGHBORHOOD) GWAS results were generated through meta-analyzing summary data from eight
574 independent datasets (3,853 POAG cases, 33,480 controls) of European ancestry from the United
575 States³⁹.

576 The Blue Mountains Eye Study (BMES) is a population-based cohort study investigating the
577 etiology of common ocular diseases among suburban residents aged 49 years or older in Australia⁵.
578 Data from 74 POAG cases and 1,721 controls of European descent with genotype information were
579 included.

580 The Progression Risk Of Glaucoma: RElevant SNPs with Significant Association
581 (PROGRESSA) study is a prospective longitudinal study of the clinical and genetic risk factors, and
582 course of early-stage glaucoma ($n = 388$). Patients with confirmed early manifest POAG on sequential
583 automated perimetry testing were consecutively recruited from ophthalmology clinics in South
584 Australia (detailed criteria in Supplementary Note). Individuals underwent six-monthly evaluation of
585 intraocular pressure, optic disc assessment, retinal nerve fibre layer analysis by optical coherence
586 tomography, and achromatic Humphrey visual field perimetry. Longitudinal data were used from all
587 visits since baseline presentation; participants were followed for one to eight years. The change in
588 retinal nerve fibre layer was measured between the baseline optical coherence tomography and the
589 most recent scan in the most-affected quadrant of the most-affected eye. Treating clinicians and
590 graders were unaware of the patient's genetic risk for glaucoma or any PRS data.

591 POAG in the ANZRAG, NEIGHBORHOOD, BMES, and PROGRESSA cohorts was defined
592 as outlined previously⁴⁰, and in accordance with the consensus statement from the World Glaucoma
593 Association⁴¹. Intraocular pressure was not used in the clinical case definition of POAG⁴¹.

594

595 **Statistical analysis.** Detailed information on the statistical analysis is provided in the Supplementary
596 Note.

597 For the VCDR (adjusted for vertical disc diameter) and intraocular pressure GWAS in UKBB,
598 we used linear mixed models (BOLT-LMM software) to account for cryptic relatedness and population
599 stratification adjusting for sex, age and the first ten principal components⁴². We meta-analyzed UKBB
600 intraocular pressure GWAS results with those from the IGGC using the inverse variance weighted
601 method (METAL software)⁴³. For the UKBB glaucoma GWAS, we removed relatives ($\pi\text{-hat} > 0.2$
602 calculated using identity by descent determined based on autosomal markers) and used PLINK
603 software for association analysis⁴⁴.

604 We then conducted a multitrait GWAS using the MTAG (version 1.0.7) software to combine
605 the European descent GWAS summary statistics from UKBB glaucoma, UKBB VCDR (adjusted for
606 vertical disc diameter), IGGC VCDR and the intraocular pressure meta-analysis (Extended Data Fig.
607 1)¹³. MTAG performs joint analysis of GWAS summary results from related traits to improve statistical
608 power to identify new genes and to maximize the predictive ability of our polygenic risk scores¹³. In
609 MTAG, GWAS summary results from related traits are used to construct the variance–covariance
610 matrix of their SNP effects and estimation error; MTAG improves the accuracy of effect estimates by
611 incorporating information from other genetic correlated traits. The MTAG method explicitly models
612 sample overlap in the input studies and provides valid estimates even when sample overlap is
613 present¹³. To benchmark the increase in effective sample size relative to just using UKBB glaucoma,
614 we calculated $(\overline{\chi^2}_{\text{MTAG}} - 1) / (\overline{\chi^2}_{\text{GWAS}} - 1)$, where $\overline{\chi^2}_{\text{MTAG}}$ and $\overline{\chi^2}_{\text{GWAS}}$ are the mean chi-
615 squared statistics from MTAG and the UKBB glaucoma analyses, respectively¹³.

616 We used a stepwise model selection procedure in the GCTA-COJO software to identify
617 independent genome-wide significant SNPs⁴⁵. Gene-based and pathway analysis were conducted in
618 MAGMA (v1.06), as implemented in FUMA (version 1.3.1)^{46,47}.

619 Prediction was based on the estimated glaucoma odds ratios (OR) from the MTAG analysis.
620 To derive a PRS, we considered a range of P -value thresholds (5×10^{-8} , 1×10^{-5} , 0.001, 0.05, 1) with
621 LD-clumping $r^2 = 0.1$ for inclusion of SNPs in the prediction model, applying each to our first prediction
622 cohort (advanced glaucoma from ANZRAG). To avoid falsely inflating prediction accuracy, we applied
623 the threshold with greatest predictive value in ANZRAG ($P \leq 0.001$) for the subsequent predictions
624 into other target sets (rather than repeatedly taking the best P -value threshold for each of the

625 datasets). We tested the LDpred⁴⁸ approach for PRS construction although the predictions were no
626 better than those from the thresholding approach described above. There was no sample overlap
627 between any of the training and target datasets (Extended Data Fig. 1).

628 Bivariate LD score regression was used to estimate the genetic correlation between pairs of
629 traits⁴⁹. The “pROC” package was used to calculate the area under the curve (AUC)⁵⁰. Analyses were
630 performed with R software⁵¹.

631

632 **Data availability.**

633 UK Biobank data are available through the UK Biobank Access Management System
634 <https://www.ukbiobank.ac.uk/>. GWAS summary statistics from the glaucoma MTAG analysis are
635 available for research uses at URL (<https://doi.org/10.6084/m9.figshare.10635854>) after publication.
636 We will return the derived data fields following the UK biobank policy and in due course they will be
637 available through the UK Biobank Access Management System.

638

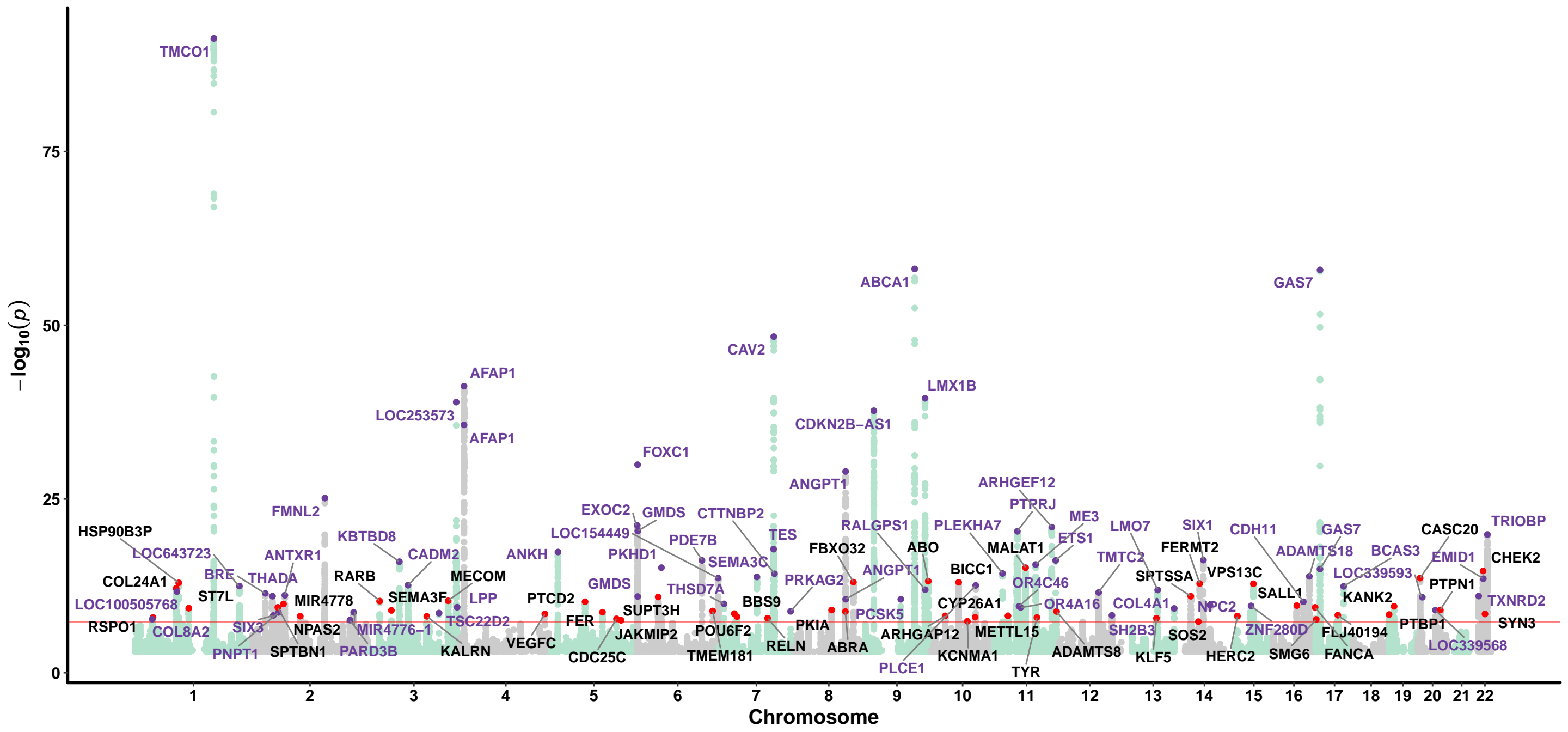
639

640

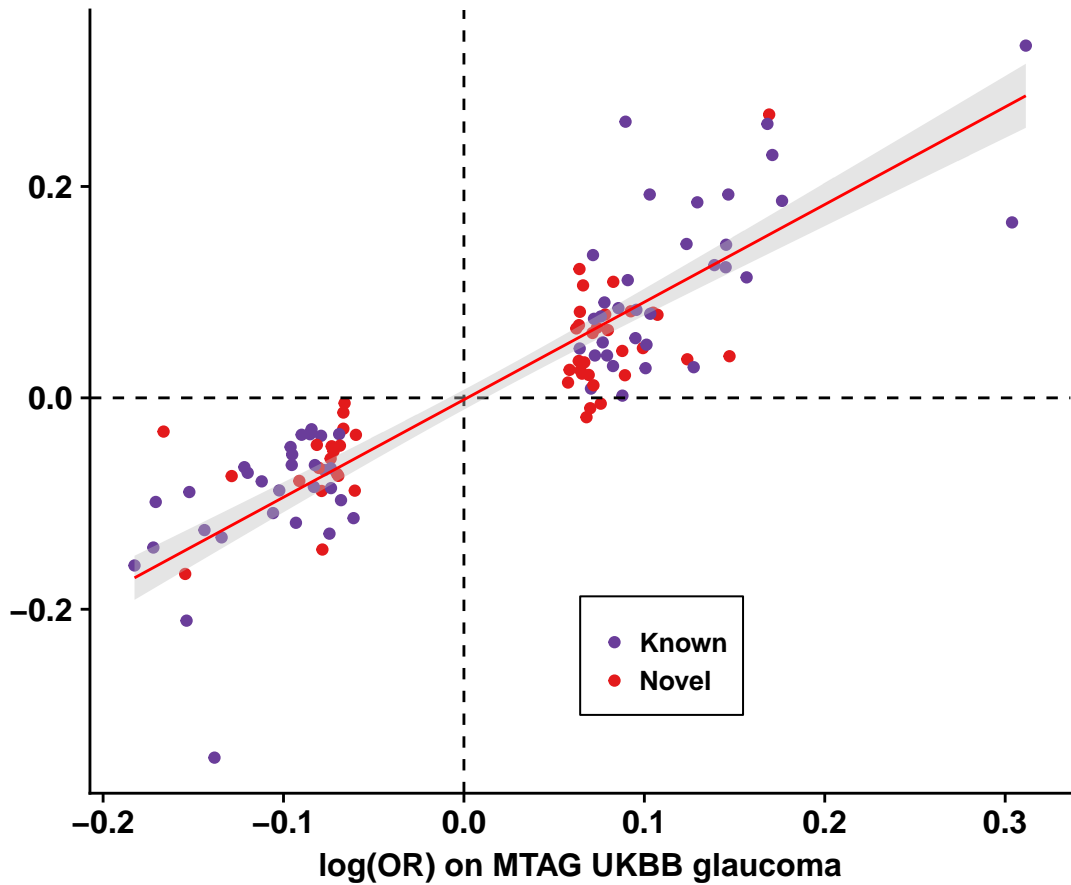
641 **Methods-only References:**

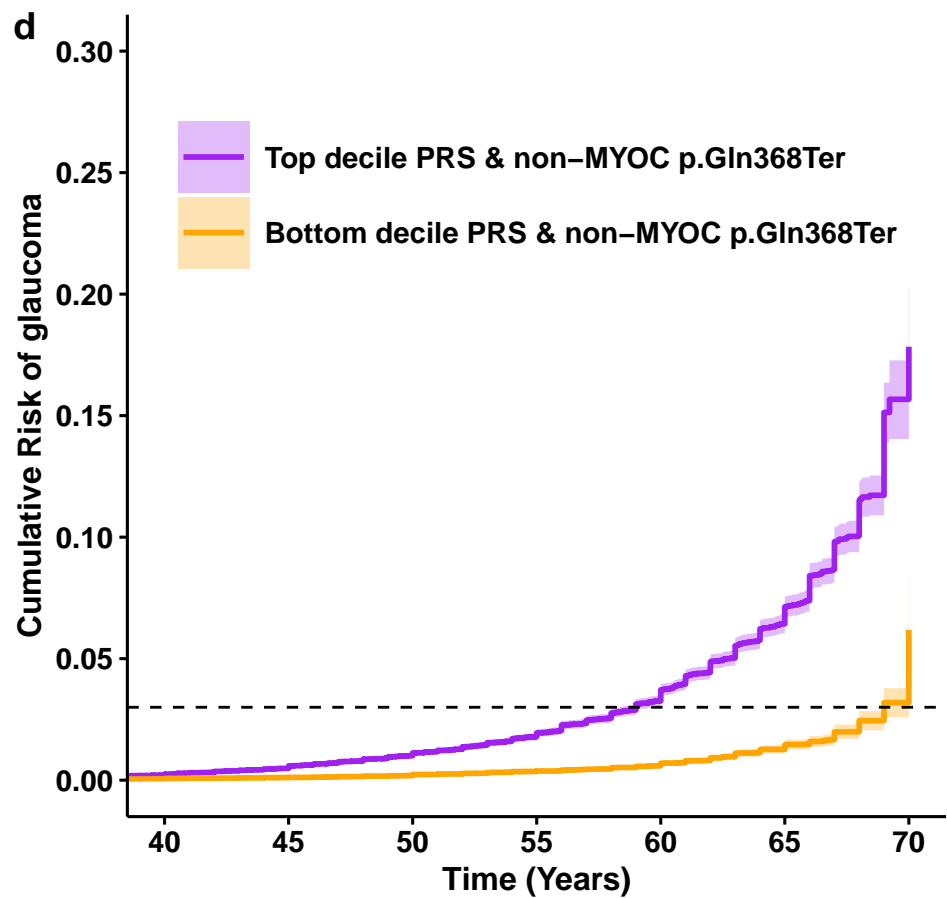
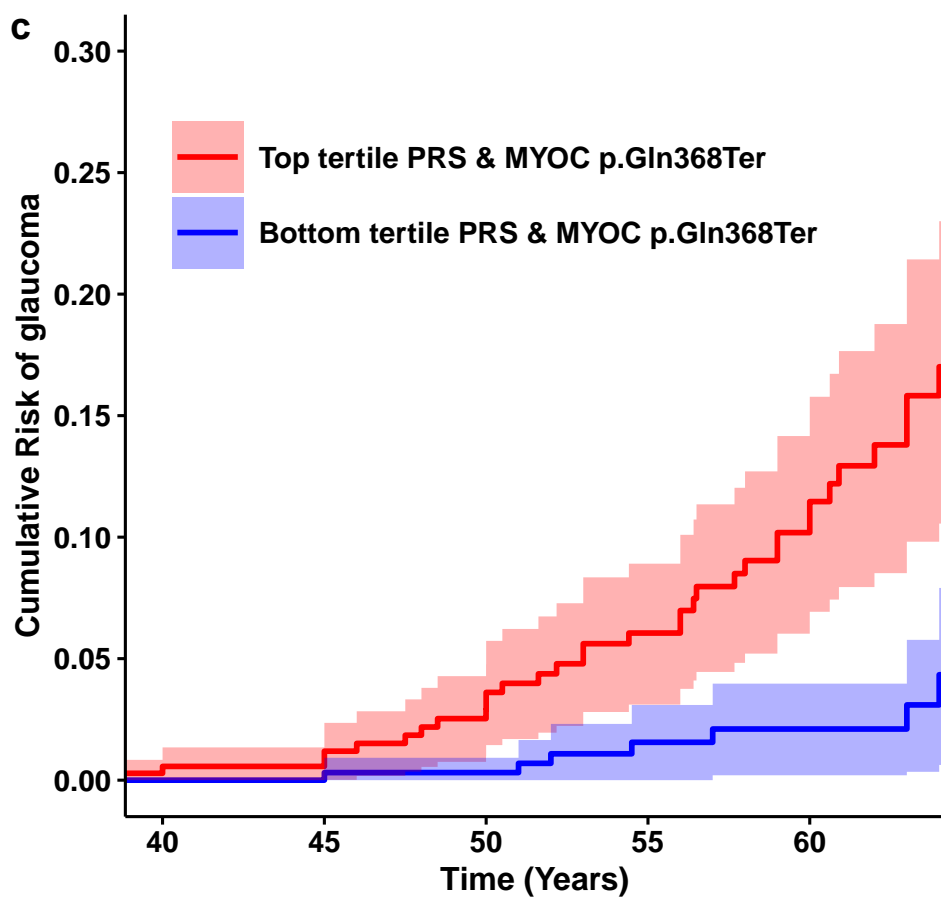
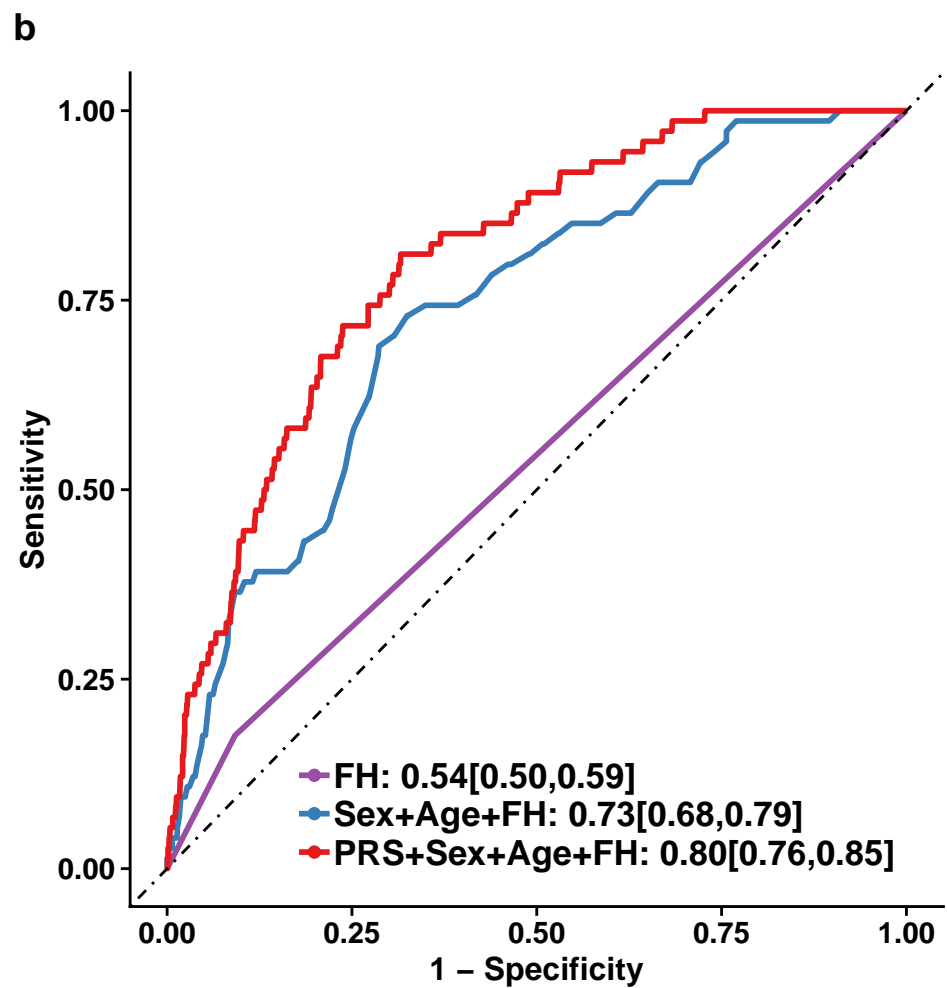
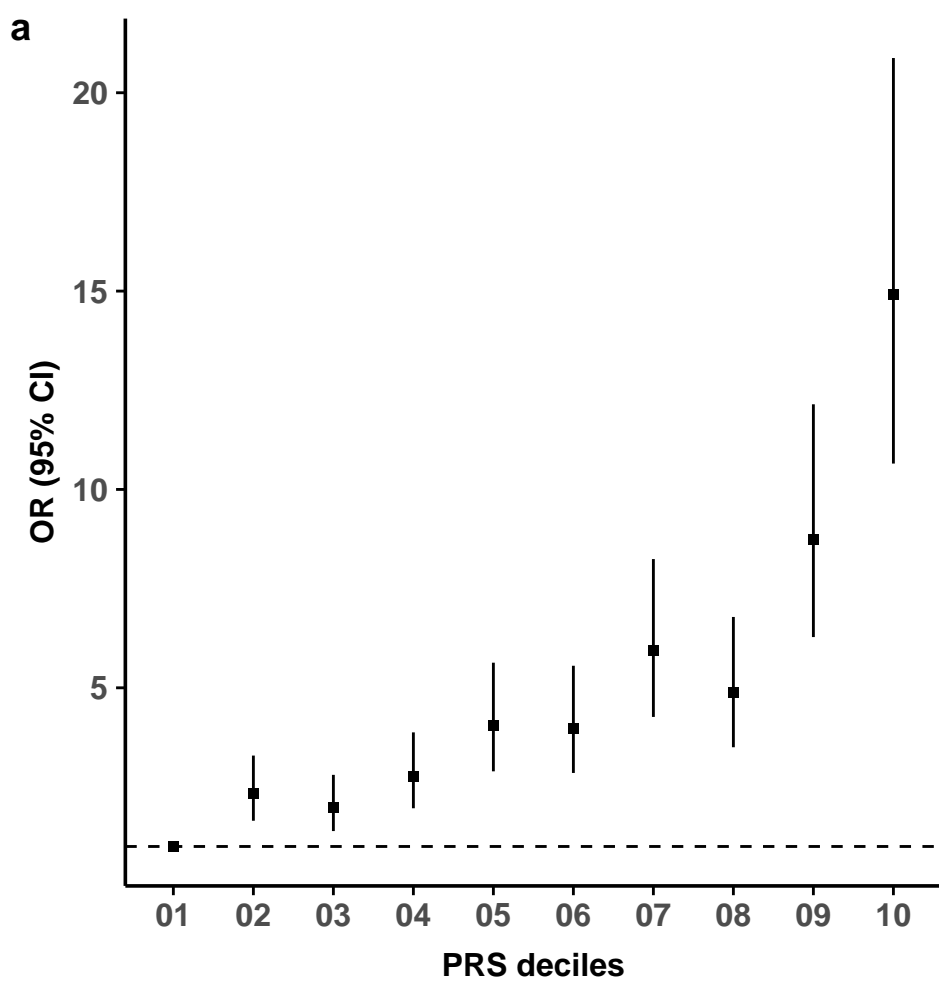
- 642 33. Bycroft, C. *et al.* The UK Biobank resource with deep phenotyping and genomic data. *Nature*
643 **562**, 203–209 (2018).
- 644 34. Han, X. *et al.* Genome-wide association analysis of 95,549 individuals identifies novel loci and
645 genes influencing optic disc morphology. *Hum. Mol. Genet.* (2019). doi:10.1093/hmg/ddz193
- 646 35. Springelkamp, H. *et al.* New insights into the genetics of primary open-angle glaucoma based
647 on meta-analyses of intraocular pressure and optic disc characteristics. *Hum. Mol. Genet.* **26**,
648 438–453 (2017).
- 649 36. Souzeau, E. *et al.* Australian and New Zealand Registry of Advanced Glaucoma:
650 methodology and recruitment. *Clin. Experiment. Ophthalmol.* **40**, 569–575 (2012).
- 651 37. Gharahkhani, P. *et al.* Common variants near ABCA1, AFAP1 and GMDS confer risk of
652 primary open-angle glaucoma. *Nat. Genet.* **46**, 1120–1125 (2014).
- 653 38. Olsen, C. M. *et al.* Cohort profile: the QSkin Sun and Health Study. *Int. J. Epidemiol.* **41**, 929–
654 929i (2012).

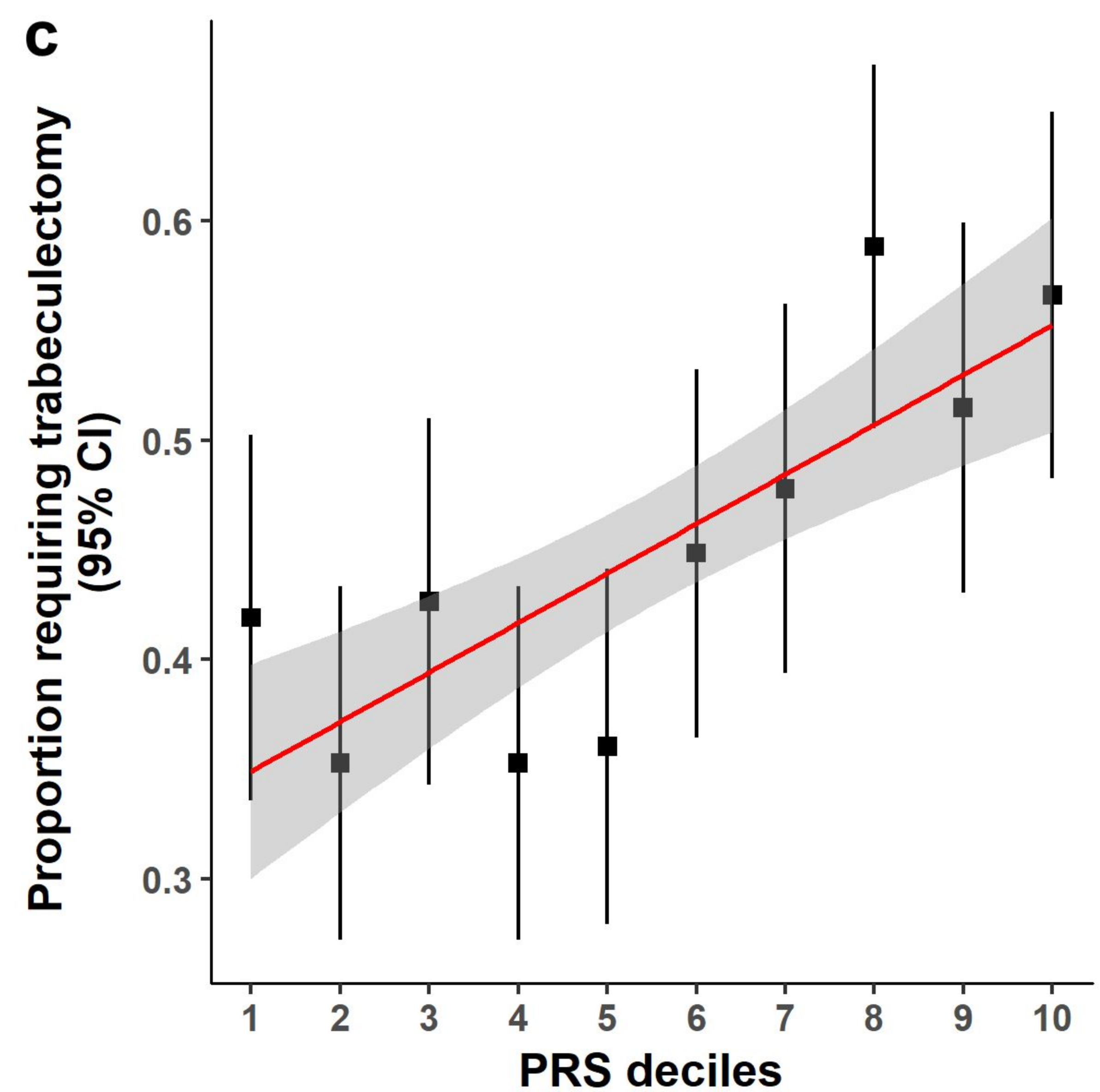
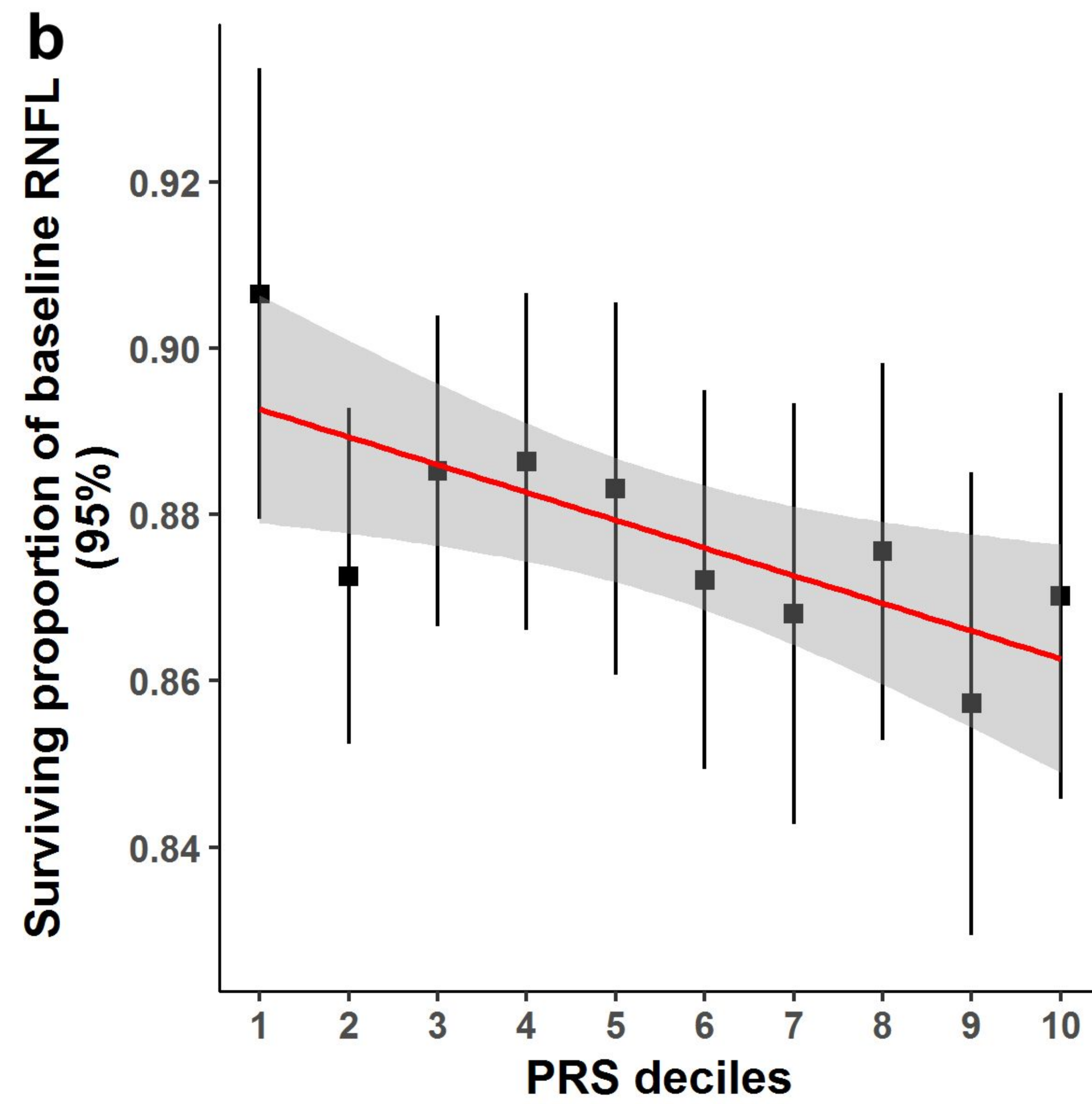
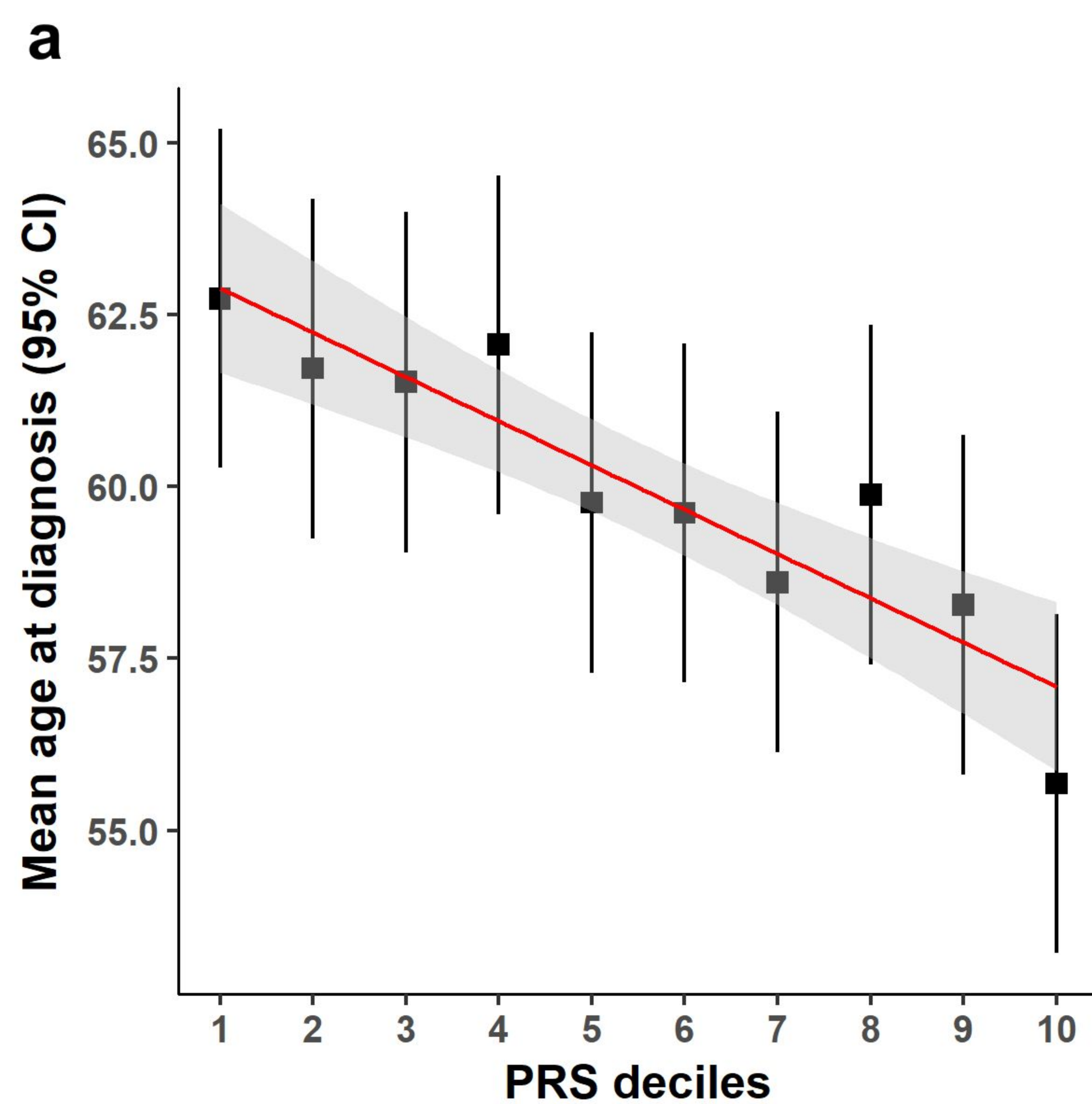
- 655 39. Wiggs, J. L. *et al.* The NEIGHBOR consortium primary open-angle glaucoma genome-wide
656 association study: rationale, study design, and clinical variables. *J. Glaucoma* **22**, 517–525
657 (2013).
- 658 40. Kwon, Y. H., Fingert, J. H., Kuehn, M. H. & Alward, W. L. M. Primary open-angle glaucoma.
659 *N. Engl. J. Med.* **360**, 1113–1124 (2009).
- 660 41. Weinreb, R. N., Garway-Heath, D. F., Leung, C., Medeiros, F. A. & Liebmann, J. *Diagnosis of*
661 *Primary Open Angle Glaucoma: WGA consensus series - 10.* (Kugler Publications, 2017).
- 662 42. Loh, P.-R. *et al.* Efficient Bayesian mixed-model analysis increases association power in large
663 cohorts. *Nat. Genet.* **47**, 284–290 (2015).
- 664 43. Willer, C. J., Li, Y. & Abecasis, G. R. METAL: fast and efficient meta-analysis of genomewide
665 association scans. *Bioinformatics* **26**, 2190–2191 (2010).
- 666 44. Purcell, S. *et al.* PLINK: a tool set for whole-genome association and population-based
667 linkage analyses. *Am. J. Hum. Genet.* **81**, 559–575 (2007).
- 668 45. Yang, J. *et al.* Conditional and joint multiple-SNP analysis of GWAS summary statistics
669 identifies additional variants influencing complex traits. *Nat. Genet.* **44**, 369–75, S1–3 (2012).
- 670 46. de Leeuw, C. A., Mooij, J. M., Heskes, T. & Posthuma, D. MAGMA: generalized gene-set
671 analysis of GWAS data. *PLoS Comput. Biol.* **11**, e1004219 (2015).
- 672 47. Watanabe, K., Taskesen, E., van Bochoven, A. & Posthuma, D. Functional mapping and
673 annotation of genetic associations with FUMA. *Nat. Commun.* **8**, 1826 (2017).
- 674 48. Vilhjálmsson, B. J. *et al.* Modeling linkage disequilibrium increases accuracy of polygenic risk
675 scores. *Am. J. Hum. Genet.* **97**, 576–592 (2015).
- 676 49. Bulik-Sullivan, B. *et al.* An atlas of genetic correlations across human diseases and traits. *Nat.*
677 *Genet.* **47**, 1236–1241 (2015).
- 678 50. Robin, X. *et al.* pROC: an open-source package for R and S+ to analyze and compare ROC
679 curves. *BMC Bioinformatics* **12**, 77 (2011).
- 680 51. R Core Team. R: A Language and Environment for Statistical Computing. (2017).



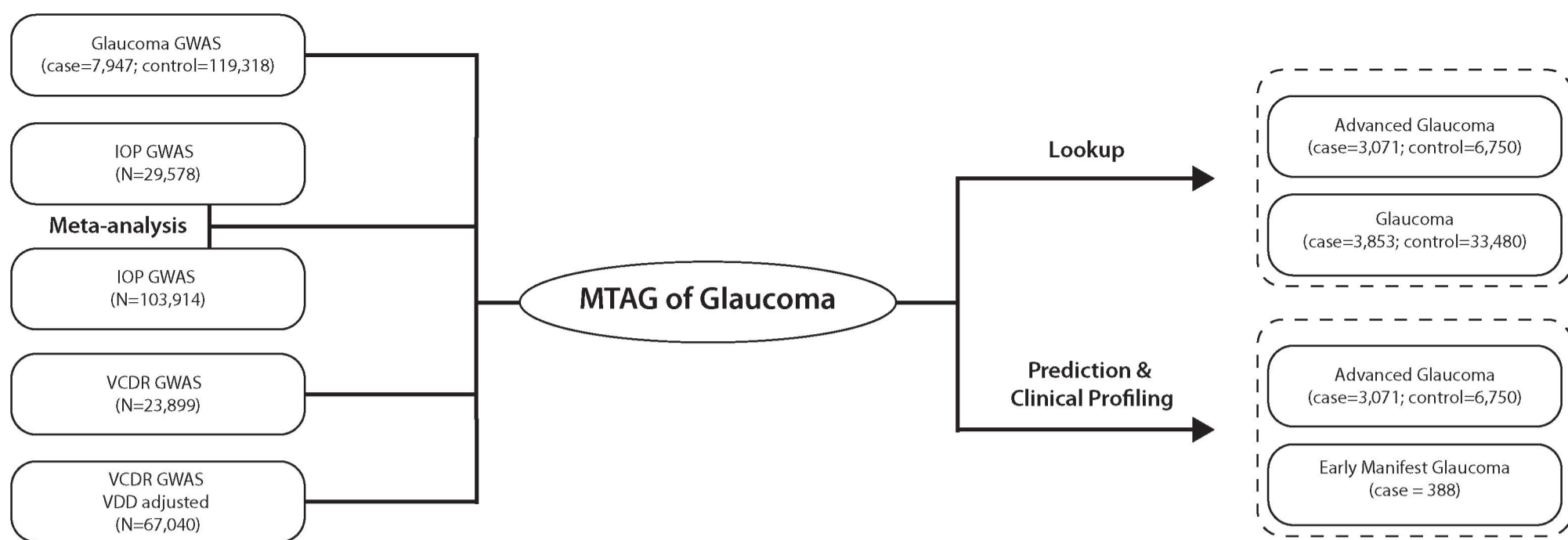
log(OR) on ANZRAG + NEIGHBORHOOD



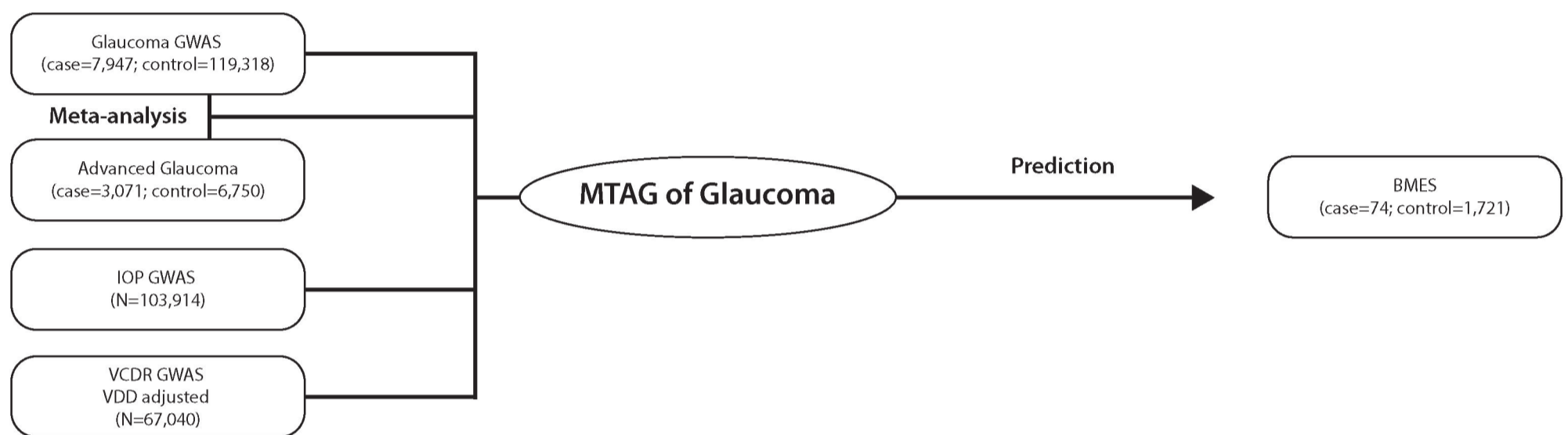




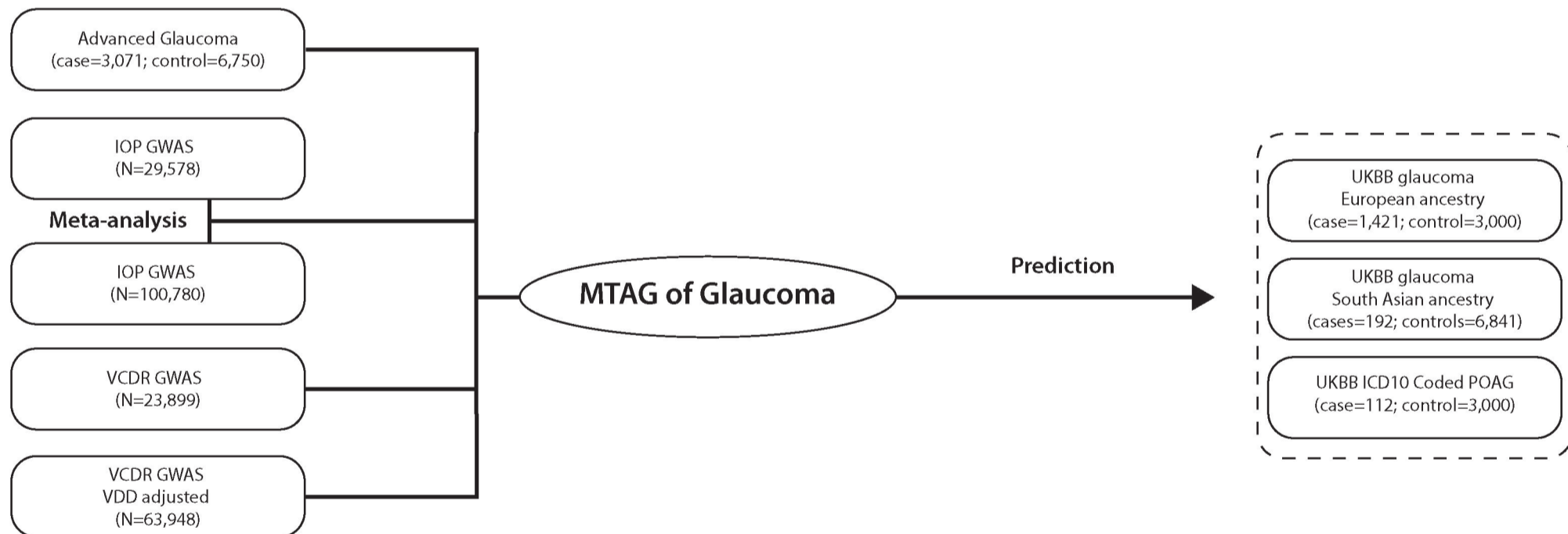
A



B



C



D

